

Introduction: Heart failure is the leading cause of death in the United States, far more commonly than all cancers combined¹. Early stages of heart failure are characterized by reduction in energy reserve with impairment of myocardial contractility and/relaxation. The PCr/ATP ratio obtained from ^{31}P MRS is a metabolic parameter used to assess myocardial energetic reserves. We propose to develop a four-channel $^1\text{H}/^{31}\text{P}$ dual-tuned transceiver array for cardiac spectroscopy at 7 Tesla. Two technical challenges need to be overcome: 1) the simultaneous decoupling of neighboring coils at two frequencies and 2) the B1 intensity fall-out in the heart region at 7T. We have developed effective solutions for both issues.

Methods: The layout of the transceiver array resembles a four-leave “clover” (Fig. 1a). At each resonant frequency, mutual decoupling was achieved by overlapping each pair of neighboring coils. The pairs of coils opposite to each other were decoupled by sharing capacitors. Thus all four coils were mutually decoupled. Dual-tuning was achieved by installing capacitors along one edge of the coil conductor for ^1H resonance and inductors along the other edge for ^{31}P resonance. In this way, high- and low-frequency currents were forced to flow along different paths. To achieve simultaneous mutual overlap decoupling, coil conductors were vertically flipped so that the magnetic fluxes generated by currents at different frequencies are equal. Fig. 1 shows the measured S_{11} of one coil when all other coils were connected. The dual-resonance and decoupling can be clearly observed.

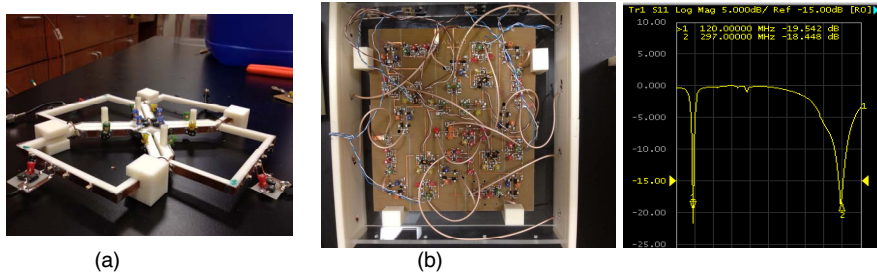


Figure 1. (a) The four-leave clover layout of the transceiver array. (b) The RF front-end of which consists of four independent sets of diplexers, T/R switches and pre-amplifiers. (c) Measured S_{11} of one coil when all other coils were connected. (d) Measured noise figure and gain of the broad band pre-amplifier.

We applied static B1-shimming with both phase and magnitude adjustment to overcome B_1^+ fall-out in the heart region at 7T². The B_1^+ field of each coil element was simulated by the FDTD with the “Hugo” human model. Simulated B_1^+ maps were then fed into a linear optimization solver with the constraint on the total RF power deposition. Figure 2 illustrates the target of the uniform excitation region and the simulated low tip-angle image as the result of B1-shimming, which is essentially the product of B_1^+ and B_1^- field. The ^{31}P Tx was implemented with equal magnitudes and appropriate 90°

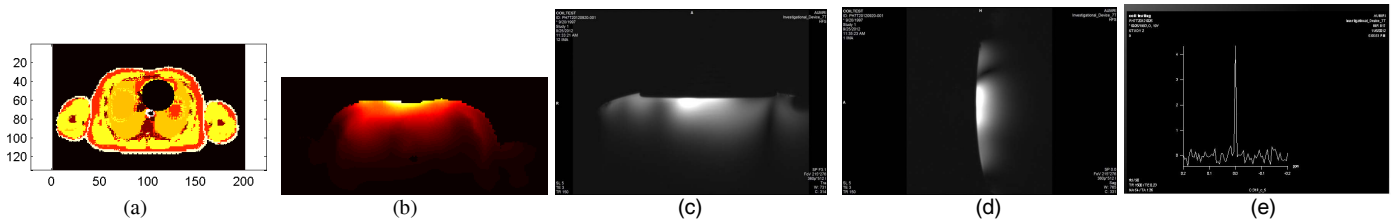


Fig. 2. (a) The “Hugo” model in simulation and the target of uniform B1 excitation at 7T. (b) The simulated low tip-angle image at 297 MHz. (c) Axial and (d) sagittal images of a saline water phantom at 7T. (e) Acquired ^{31}P signal at 7T from a phosphate buffer phantom using a free induction decay

phase shifts, so that a circularly polarized field can be generated at the center of the coil array. Dedicated RF pre-amplifiers were also developed for 120MHz and 297MHz receive signal amplification. The noise-figure was 0.88 dB and 0.58 dB and the gain was 28.7 dB and 29.5 dB at 120 MHz and 297 MHz respectively. The RF front-end is illustrated in Fig. 1b. It consists of four independent units. Each unit has its own diplexer and T/R switches. The Tx ends of the T/R switches were connected to a bank of power dividers and phase shifters, which implemented B1-shimming.

Results and Discussion: The transceiver array and its front-end were fabricated in-house and tested on a MAGNETOM 7T scanner (Siemens Healthcare, Erlangen, Germany) and a saline water phantom having the same size as a human chest. Figure 2 shows the initial phantom test results. A gradient echo sequence was applied with a nominal tip-angle of 20°. Scanning parameters were TR=150ms, TE=3 ms and 1 average. The long TR was intentionally used to generate brighter images to illustration purposes. Images were acquired with TR as short as 8 ms without artifacts. It can be seen that the acquired axial image closely resembles the simulated low tip-angle image despite the large geometric difference between the “Hugo” model and the water phantom. No B1 fallout was observed in the heart region. These results indicate that the static B1-shimming derived from simulated electromagnetic field is generally valid. In addition, good field coverage on the sagittal slice was observed. We also tested the transceiver array with a small (half liter) bottle of phosphate buffer solution without re-tuning the coils. Despite this significant mismatching condition, good signal was detected and shown in Fig. 2e.

Conclusions: We developed a 4-channel $^1\text{H}/^{31}\text{P}$ dual-tuned transceiver array and the front-end for cardiac spectroscopy at 7 Tesla. Initial proton images demonstrate good field coverage by static B1 shimming and initial tests of ^{31}P signals are promising. Currently we are waiting to test it on human subjects.

References: 1) Schiros, CG, et.al. Circulation, (2012): 125:19:2334-42 2) van den Bergen B, et.al, Phys. Med. Biol. (2007):52: 5429-41